Cancer Letters 470 (2020) 18–28

Contents lists available at ScienceDirect

Cancer Letters

journal homepage: www.elsevier.com/locate/canlet

Original Articles

Acidosis-induced metabolic reprogramming in tumor cells enhances the anti-proliferative activity of the PDK inhibitor dichloroacetate

C.A. Schoonjans[a,b], N. Joudiou[c], D. Brusa[d], C. Corbet[b], O. Feron[b], B. Gallez[a,*]

[a] Université Catholique de Louvain (UCLouvain), Louvain Drug Research Institute, Biomedical Magnetic Resonance Research Group, Brussels, Belgium
[b] Université Catholique de Louvain (UCLouvain), Institut de Recherche Expérimentale et Clinique, Pole of Pharmacology and Therapeutics, Belgium
[c] Université Catholique de Louvain (UCLouvain), Louvain Drug Research Institute, Nuclear and Electron Spin Technologies, Brussels, Belgium
[d] Université Catholique de Louvain (UCLouvain), Institut de Recherche Expérimentale et Clinique, Flow Cytometry Platform, Belgium

ARTICLE INFO

Keywords:
pHe
13C-NMR
Glycolysis inhibition
Metabolic plasticity
Bioenergetics

ABSTRACT

Altered metabolic pathways in cancer such as exacerbated glycolytic flux and increased glutamine metabolism are promising targets for anti-cancer therapies. While commonly observed in glycolytic tumors, extracellular acidosis has never been considered as a potential modulator of anti-metabolic drug activity such as dichloroacetate (DCA). Using cancer cells from various origins selected for their ability to proliferate under acidic conditions, we found that DCA exerts greater inhibitory effects on the growth of these acid-adapted cells than in parental cells. Moreover, daily DCA administration to mice led to a significant decrease in tumor growth from acid-adapted cells but not from parental cells. 13C-tracer studies revealed that DCA induced a double metabolic shift, diminishing glycolysis and increasing intracellular glutamine in acid-adapted cells. As a consequence, DCA reduced the pentose phosphate pathway activity more extensively and increased apoptosis in acid-adapted cells. Finally, the combination of DCA with a glutaminase inhibitor significantly enhanced the cytotoxic effects of DCA. Overall, the interplay between acidosis and DCA exposure leads to metabolic reprogramming that considerably alters cellular fitness.

1. Introduction

Glucose fermentation through glycolysis even in the presence of oxygen (aerobic glycolysis) is a common feature of malignant tumors and is associated with cancer aggressiveness and invasion [1,2]. This exacerbated glycolytic flux is an enticing target for treatments because of their specificity to cancer cells. Indeed, upregulated glycolysis is described as an effective way for cancer cells to support rapid proliferation, an adaptation that is not present in most normal cells [3,4]. To date, clinical studies with glycolysis inhibitors have provided encouraging data [5,6] but efforts are still needed to identify which tumors will benefit from these treatments. Among glycolytic modulators, inhibitors of pyruvate dehydrogenase kinase (PDK) have received particular attention [7–9]. PDK inactivates the enzyme pyruvate dehydrogenase (PDH) by phosphorylation. The active unphosphorylated PDH converts pyruvate to acetyl-CoA that fuels the tricarboxylic acid cycle (TCA). Therefore, the inhibition of PDK reactivates PDH leading to a redirection of glucose metabolism from cytoplasmic glycolysis to mitochondrial oxidation [10].

It has been repeatedly observed that dichloroacetate (DCA), a PDK inhibitor currently tested in clinical studies (i.e. Trial ID: NCT01386632 and ACTRN12615000226505), decreases the proliferation of various cancer cells lines [11–14]. DCA reverses aerobic glycolysis leading to a decrease in lactate production. In addition, by reactivating the mitochondrial function, DCA reverses the suppression of mitochondria-dependent apoptosis [12,15]. Finally, DCA decreases glycolytic intermediates available for anaplerosis, in particular through the pentose phosphate pathway [12]. Consequently, this reduction of building blocks from glycolysis accounts for the anti-proliferative effects of PDK inhibition [16]. Besides these direct metabolic effects, it has been shown that DCA decreases HIF-1 alpha activity and increases p53 activity resulting in decreased glucose uptake, tumor angiogenesis, tumor perfusion and tumor growth [12,17,18]. In addition, a survey of studies on DCA from Papandreou et al. highlighted that DCA was more effective *in vivo* than *in vitro* [19]. These observations suggest that factors of the tumor microenvironment may modulate the efficacy of DCA.

Because the exacerbated glycolytic flux in tumor leads to extracellular acidosis, it is crucial to investigate the effect of cell adaptation to acidosis on DCA activity [20,21]. Indeed, besides its contribution to tumor genomic instability and invasiveness [22–24], extracellular

* Corresponding author. Biomedical Magnetic Resonance, UCLouvain, Avenue Mounier 73.08, B-1200, Brussels, Belgium.
E-mail address: bernard.gallez@uclouvain.be (B. Gallez).

https://doi.org/10.1016/j.canlet.2019.12.003
Received 19 September 2019; Received in revised form 20 November 2019; Accepted 1 December 2019

acidosis can lead to tumor metabolic reprogramming [25–27]. For example, it was recently demonstrated that a long-term exposure of cancer cells to acidic pH leads to a metabolic reprogramming towards glutamine metabolism at the expense of the glycolytic metabolism [28,29].

The aim of our study was to unravel the role of extracellular acidosis on the efficacy of DCA. On one hand, because of its mode of action, DCA should theoretically target aggressive glycolytic tumors. On the other hand, the extracellular acidosis associated with glycolysis is responsible for a metabolic shift from glycolysis to glutamine metabolism: this metabolic reprogramming could render cells adapted to low extracellular pH (pHe) less sensitive to DCA because they are less dependent on glycolysis. Considering these theoretical contradictory effects, we aimed to examine how acidic pH influenced the effects of DCA on the bioenergetics and proliferation of cancer cells. We used a long-term selection of cancer cells able to proliferate under acidic conditions [28]. We first observed that DCA was more effective in acidic pH-adapted cells compared to their native counterparts in reducing cell viability, cell proliferation and tumor growth. To dissect the mechanisms responsible for this enhanced effect, we assessed the uptake of DCA by the tumor cells, the PDK isoforms abundance and the phosphorylation of PDH by PDK. Via ^{13}C NMR spectrometry, we measured metabolic shifts induced by DCA in glucose and glutamine metabolism. To further investigate the link between metabolic shift and their action on growth and proliferation, we measured pentose phosphate pathway activity and mitochondrial dependent apoptosis. Finally, we assessed the relevance of our results by performing a combined therapy with DCA and glutaminase inhibitors. Overall, we discovered that the metabolic plasticity observed under acidosis can be exploited to enhance the activity of PDK inhibitors.

2. Material and methods

2.1. Cell culture and reagents

All cell lines were acquired from the American Type Culture Collection (ATCC, Manassas, VA, USA). Cells were stored according to the supplier's instructions and used within 6 months after defrosting frozen aliquots. SiHa cervix cancer cells and HCT-116 colon cancer cells were maintained in DMEM supplemented with 10 mM of glucose, 2 mM of glutamine (Sigma-Aldrich, Saint-Louis, MO, USA), 10% heat-inactivated FBS (Thermo Fisher Scientific, Waltham, MA, USA) and with 25 mmol/L of both PIPES and HEPES to adjust pH to 7.4 or 6.5. Acidic pH-adapted tumor cells were established as previously described by Corbet et al. [28]. Briefly, SiHa and HCT-116 cell lines were cultured in DMEM medium (supplemented with 10 mM of glucose, 2 mM of glutamine, 10% heat-inactivated FBS and with 25 mmol/L of both PIPES and HEPES) buffered at pH 6.5. 72 h of incubation in the 6.5 medium led to a significant inhibition of tumor cell growth. Tumor cells were maintained in this medium (repeatedly renewed) for 8–10 weeks until they completely recovered and grew at the same rate as parental cells. Dichloroacetate (DCA) and 6-Aminonicotinamide (6-AN) were purchased from Sigma-Aldrich and were directly dissolved in culture media. Bis-2-(5-phenylacetamido-1,3,4-thiadiazol-2-yl)ethyl sulphide (BPTES) was purchased from Sigma-Aldrich and first dissolved in DMSO and then diluted in culture media.

2.2. Cell density

Cell density was assessed by using the Presto Blue reagent (Thermo Fisher Scientific, Waltham, MA, USA) according to manufacturer's instructions. Four cancer cell types were analyzed: parental cells cultured at a pH of 7.4 or acutely exposed to an acidic pH (pH 6.5; 48h) and chronically acid-adapted cells cultured at a pH 6.5 or exposed to a pH 7.4 for 24 or 48 h. Cells were treated with 0, 5 or 10 mM of DCA. For the combined study, cells were treated with 0, 1 or 5 mM of DCA in presence or not of 10 μM BPTES. 48 h after, 10% Presto Blue reagent was added to each well. After 1 h at 37°-C, fluorescence intensity (λ_{exc}/λ_{em} = 544/612 nm) was measured using a plate reader (SpectraMax M2e, Molecular Devices), which allowed the quantification of cell viability by using the reducing power of living cells.

2.3. Cell proliferation

Cell proliferation was assayed with a 5-bromo-2′-deoxyuridine (BrdU)-ELISA based kit (Roche, Bâle, Switzerland) following the provider's instructions. Cells were treated with 0, 5 or 10 mM of DCA. After treatment for 48 h, cells were incubated in the presence of BrdU for 2 h. The amount of BrdU incorporated in the cells was assessed by measuring the absorbance at 370 nm using a plate reader (SpectraMax M2e, Molecular Devices), which allowed the quantification of DNA synthesis in replicating cells.

2.4. Western blotting analyses of PDK isoforms and PDH phosphorylation

Whole cell lysates were collected and subjected to immunoblot analysis as previously described [30]. Primary antibodies: PDHK1 (1:1000,#3820, Cell Signaling, Danvers, MA, USA), phospho-PDHE1-A (1/1000, #ABS204, Millipore, Burlington, MA, USA), PDK1 (1/1000, #3205, Cell Signaling), PDK2 (1/1000, WH0005164M2, Sigma), PDK3 (1/1000, NBP1-32581, Novus, Saint Charles, MO, USA) and PDK4 (1/1000, NBP1-07047, Novus). Gel loading was normalized with a HSP90 antibody (1/1000, 610419, BD Bioscience, San Jose, CA, USA).

2.5. ^{13}C NMR spectroscopy measurement of intra/extracellular metabolites

Intra- and extracellular metabolites were measured with ^{13}C nuclear magnetic resonance (NMR) via the use of ^{13}C-labeled tracers. 1×10^6 cells were seeded in 100 mm dishes for Glucose-$^{13}C_6$ tracer experiments and 2×10^6 cells were seeded in 150 mm dishes for Glutamine-$^{13}C_5$ tracer experiments (two dishes per condition). After 24 h, cells were cultured with or without 5 mM DCA and with DMEM supplemented with either 10 mmol/L of D-Glucose-$^{13}C_6$ (CLM-1396, Euriso-top, Saint-Aubin, France) and 2 mmol/L of unlabeled L-glutamine, or 10 mmol/L of unlabeled D-glucose and 2 mmol/L of L-Glutamine-$^{13}C_5$ (CC1050P1, Cortecnet, Voisins-le-Bretonneux, France). 24h after treatments, extracellular media were collected and polar cellular metabolites were extracted using dual phase extraction procedure adapted from Teng et al. [31]. Briefly, a mixture of methanol, chloroform and water in the volume ratio 2:2:1 was used to generate two-phase extracts after centrifugation. The upper aqueous phase containing polar metabolites was collected. The solvent was completely removed using a vacuum concentrator. The sample was reconstituted in 600 μl sodium phosphate buffer with 10% deuterium oxide containing 0.75 wt % 3-(trimethylsilyl)propionic-2,2,3,3-d_4 acid (TSP) (Sigma-Aldrich, 293040). For extracellular metabolites, 540 μl of media was used and 60 μl of deuterium oxide containing 0.75 wt % TSP was added. ^{13}C NMR spectra of cellular extracts and media were acquired on a 600 MHz Bruker NMR equipped with a broadband cryoprobe. The acquisition time was 0.8 s with 1024 repetitions for Glucose-$^{13}C_6$ tracer and 2048 repetitions for L-Glutamine-$^{13}C_5$ and 10 s of interpulse delay (1D sequence with inverse gated decoupling using 30° flip angle). Spectrum analysis, assignment and quantification were performed with Topspin and MestReNova software. For Glutamine-$^{13}C_5$ tracer extra dishes were seeded for protein normalization (Pierce™ BCA Protein Assay Kit, Thermo Fisher).

2.6. Measurement of oxygen consumption rate

The effect of DCA on oxygen consumption rate (OCR) was evaluated on parental and acid-adapted cell lines via a X-band Electron Paramagnetic Resonance (EPR) spectrometer operating at 9 GHz

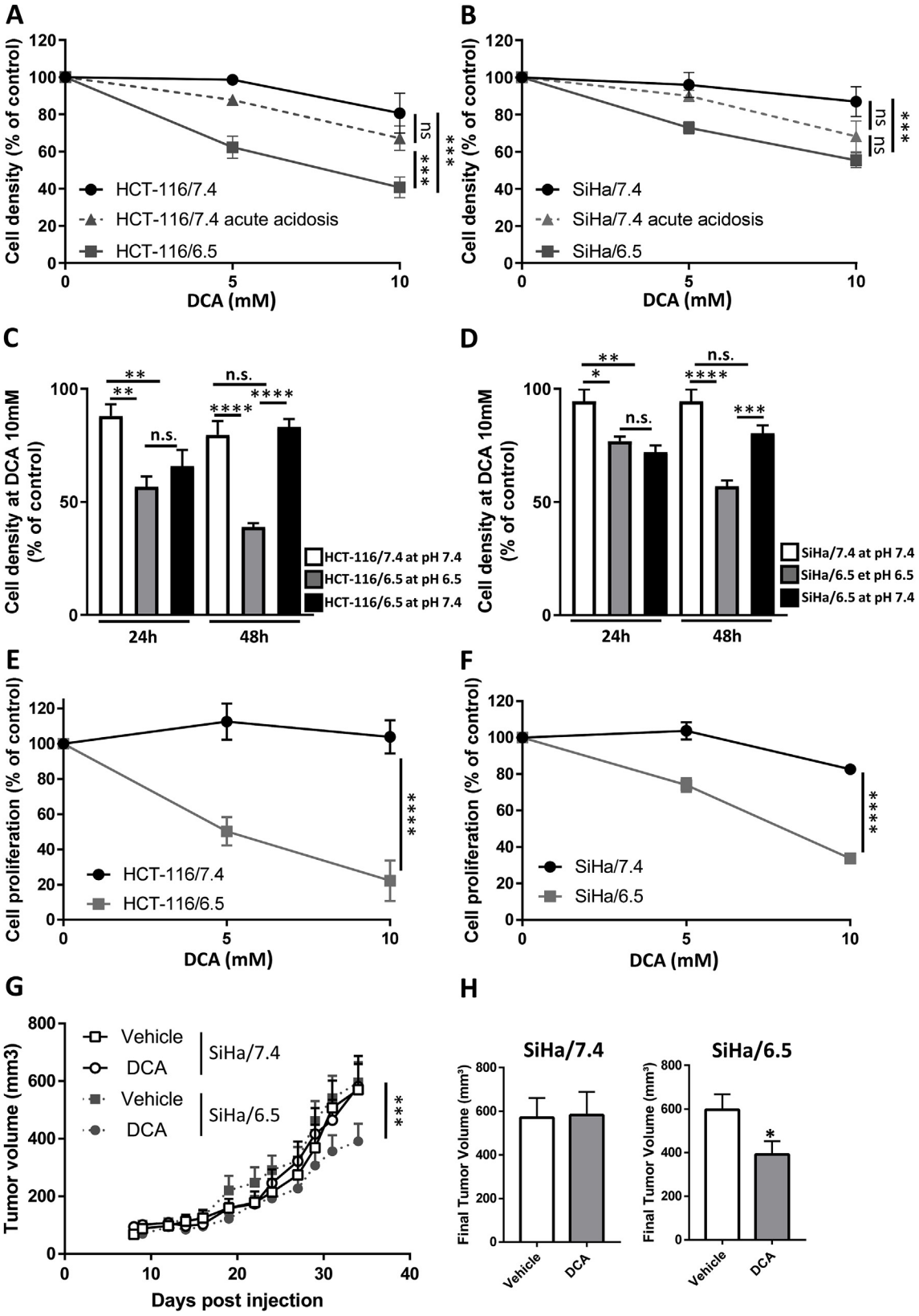

Fig. 1. Chronic acidosis enhances the growth inhibitory action of DCA. A-B, effect of increasing doses of DCA (0-5-10 mM) on cell density (A, HCT-116 cells and B, SiHa cells) after 48 h exposure (n = 3). C-D, acid adapted cells were incubated at pH 7.4 for 24 and 48 h. Cell density measurement (C: HCT-116 cell lines and D: SiHa cell lines) after DCA treatment (10 mM, 24 and 48 h) of parental (white), acid-adapted cells (gray) and acid-adapted cell cultured at pH 7.4 (black) (n = 3). E-F, effect of increasing doses of DCA (0-5-10 mM) on cell proliferation (E, HCT-116 cell lines and F, SiHa cell lines) after 48 h exposure (n = 3). G, tumor growth of SiHa parental and SiHa acid-adapted xenografts in nude mice (n = 8–10) treated daily with or without DCA (100 mg/kg). H, Final tumor volume of SiHa/7.4 and SiHa/6.5 xenografts. Statistical analysis: Two-way ANOVA Sidak's multiple comparisons test (A–G) and unpaired *t*-test (H). *p < 0.05, **p < 0.01, ***p < 0.001, ****p < 0, 0001.

(Bruker EMXplus) as previously described [32]. Cells were incubated with 5 mM of DCA for 24h; after trypsinization, cells were resuspended in cell growth medium at a concentration of 2.5 × 10^6 cells/mL. 100 µL of cell suspension were mixed with 100 µL of 20% w/v of dextran in 0.9% NaCl solution and 6 µL of 0.2 mM ^{15}N-PDT, which served as oxygen sensor. A 75 µL-glass capillary tube (Hirschmann Labogeräte) was filled with the cell suspension, sealed and inserted into a quartz tube, then placed into the EPR cavity. The cavity was continuously flushed with a gas mixture (400 l/h) at 37 °C throughout the spectra acquisition. EPR spectra were acquired every 60 s, and pO_2 values were obtained by measuring the peak to peak EPR signal linewidths, which was then converted into pO_2 by means of a calibration curve. Oxygen consumption rate (OCR) was then calculated as the slope of pO_2 over time curve.

2.7. DCA uptake measurement

Cells were treated with or without 5 mM DCA. 24 h after treatment, extracellular media was collected and proteins were extracted and quantified (Pierce™ BCA Protein Assay Kit, Thermo Fisher Scientific) for sample normalization. Collected extracellular media was processed and analyzed by ^{13}C NMR spectroscopy as described in the previous section. DCA chemical shift of the carbon from the carboxylic group was found at 173.56 ppm.

2.8. NADPH and NADP$^+$ measurements

Cells were treated with or without 5 mM DCA and with or without 0.1 mM 6-aminonicotinamide (6-AN) for 48 h. NADPH and NADP$^+$ levels were detected individually from 12,000 harvested cells using the NADP/NADPH-Glo Assay kit (Promega, Leiden, Netherlands) according to manufacturer's instructions.

2.9. Flow cytometry

After treatment with or without 10 mM DCA for 48 h, cells were rinsed with PBS, detached with trypsin and resuspended in fresh media. EBioscience™ Annexin V Apoptosis Detection Kit APC (Invitrogen™, Thermo Fisher Scientific) was used for the determination of the percentage of living, apoptotic and dead cells following provider's instructions. The cells were distinguished between alive (double negative) and dead: early/medium apoptotic (AnnV + DAPI−), late apoptotic (AnnV + DAPI+). Flow cytometric data were acquired using a BD FACS Canto II flow cytometer and processed with FlowJO software. FACS analysis by FlowJo was processed for each cell line separately. At least 20,000 events were analyzed for each sample.

2.10. Mass spectrometry

Cells were washed with PBS before adding culture media containing 2 mM L-[U–^{13}C]glutamine tracer for 24 h. Tumor cells were rinsed in cold 0.9% NaCl and snap-frozen in liquid nitrogen. Mass spectrometry measurements (^{13}C isotope analysis and absolute quantification of intracellular metabolites) were then performed by the Metabolism Core in the Sanford Medical Discovery Institute (La Jolla) [33].

2.11. In vivo tumor growth

Animal studies were undertaken in accordance with Belgian and the Université catholique de Louvain ethical committee regulations (agreement numbers 2018/UCL/MD/021). A total of 2.10^6 native SiHa cells or acidic pH-adapted SiHa cells were inoculated subcutaneously into the right flank of six-week-old female NMRI nude Mice (Janvier, Le Genest-Saint-Isle, France). Tumors were measured three times per week with an electronic caliper. When they reached a mean diameter of 5 mm, DCA in PBS (100 mg/kg) or PBS alone was injected daily intraperitoneally.

2.12. Statistical analysis

Data are expressed as mean ± SEM (standard error of the mean). The number of experiments and the statistical test used are given in each figure caption. All data were analyzed with the GraphPad Prism 8.0 software.

3. Results

3.1. Chronic acidosis enhances the growth inhibitory action of DCA

We first examined whether extracellular acidosis could influence the effects of DCA on cancer cell growth. We investigated possible changes on cell density and cell proliferation under DCA treatment in acid-adapted HCT-116 and SiHa cancer cells in comparison to native (parental) counterparts. The effect of increasing doses of DCA on cell density was significantly more pronounced in acid-adapted cells compared to corresponding parental cells (Fig. 1A–B). In contrast, in cells acutely exposed to acidosis, DCA did not induce any significant effect on cell density: cell density was not significantly different between parental cells under physiological pH and under acute acidic pH (Fig. 1A–B). We investigated the reversibility of the increased sensitivity to DCA resulting from chronic exposure to acidic pH. For that purpose, HCT-116/6.5 and SiHa/6.5 cells were cultured at pH 7.4 for 24 and 48 h. After 24 h of DCA treatment at pH 7.4, there was no significant difference between acid-adapted cells cultured at pH 6.5 and 7.4. However, after 48 h h, acid-adapted cells cultured at pH 7.4 presented the same sensitivity to DCA than parental cells (Fig. 1 C-D). The effect of increasing doses of DCA on cell proliferation was also significantly more pronounced in acid-adapted cells compared to corresponding parental cells (Fig. 1E–F). Exposition to 10 mM DCA induced a reduction in cell proliferation by 78% and 66% in acid-adapted HCT-116 and SiHa cells, respectively but either was not or barely effective in parental cells. To assess the therapeutic relevance of our *in vitro* experiments, we monitored the *in vivo* effect of DCA on the growth of tumors obtained by injection of parental or acid-adapted SiHa cells in mice. Daily administration of DCA (100 mg/kg) had no effect on parental SiHa tumors. In contrast, DCA treatment led to a significant decrease in tumor growth obtained from acid-adapted SiHa cells (Fig. 1G–H).

3.2. The higher uptake of DCA and the lower expression in PDK isoforms in acid-adapted cells account for the larger decrease in PDH phosphorylation

We first confirmed that the effects observed on cell density and proliferation were related to PDK inhibition, i.e. to a decrease in phosphorylated PDH. For both cell lines exposed to 5 mM DCA, a decrease in phosphorylated PDH was observed, and this reduction was more important in acid-adapted cells compared to parental cells (Fig. 2A). Of note, in untreated SiHa cells, the basal level of phosphorylated PDH was lower in acid-adapted cells compared to parental cells (Fig. 2A, right panel). We further explored the possible mechanisms responsible for this higher activity of DCA in acid-adapted cells. We first found that the DCA uptake, as quantified by ^{13}C NMR spectrometry, was significantly higher in acid-adapted cells than in parental cells (Fig. 2B). We also quantified the expression of the four different PDK isoforms in parental and acid-adapted cells. We observed that, except for PDK1 in HCT-116 cells, the abundance of each PDK isoform was reduced in acid-adapted cells compared to parental cells (Fig. 2C). This reduction in the pool of PDK as well as the higher uptake of DCA in acid-adapted cells is very likely to contribute to the larger decrease in PDH phosphorylation induced by DCA in acid-adapted cells.

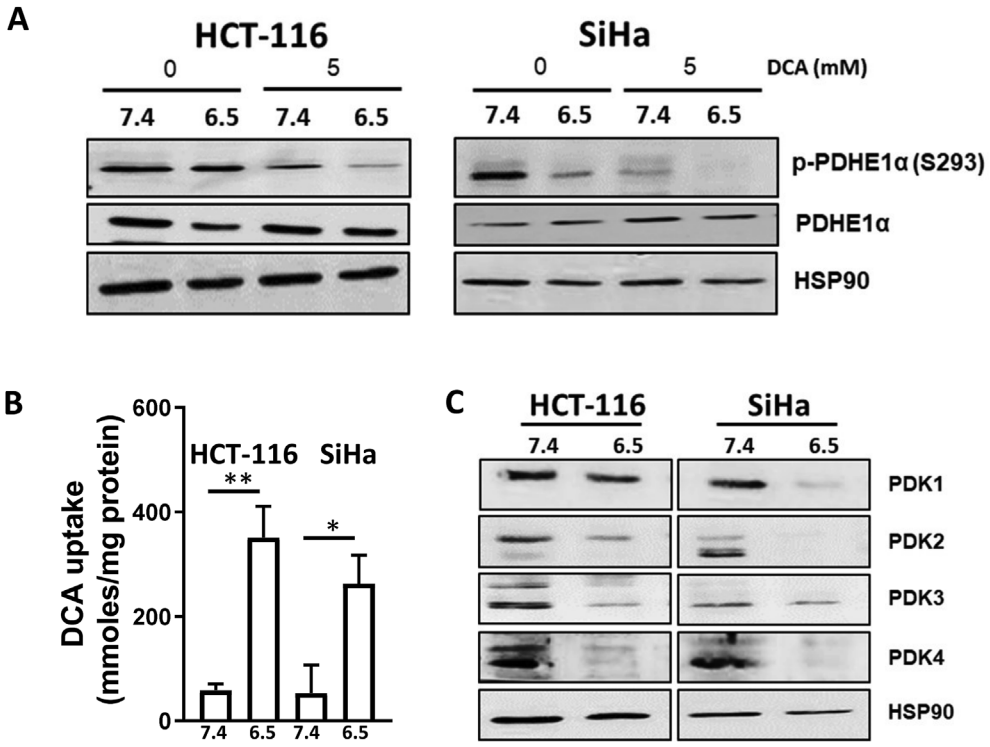

Fig. 2. Higher uptake of DCA and lower PDK abundance in acid-adapted cells account for the DCA-induced decrease in phosphorylated PDH. A, representative immunoblotting of phosphorylated and total form of PDH in SiHa, HCT-116 parental cell lines and acid–adapted cells after exposure to 0 or 5 mM of DCA for 24 h (n = 3). B, DCA uptake after exposure to 5 mM DCA for 24 h (n = 4) of SiHa and HCT-116 cell lines as well their adapted-cells. One-way ANOVA Sidak's multiple comparisons test, *p < 0.05, **p < 0.01. C, representative immunoblotting of the four PDK isoforms in SiHa, HCT - 116 cell lines and their pH 6.5 (n = 2).

3.3. The "glycolysis to oxidative" metabolic shift induced by DCA is larger in acid-adapted cells

^{13}C NMR spectrometry was further used to assess the effect of DCA on glucose metabolism in parental and acid-adapted cells. These two parental cell lines are known to present different metabolic profiles. The glucose consumption is two times higher in HCT-116 than in SiHa cells (8 μmol/10^6 cells vs 4 μmol/10^6 cells) and lactate secretion is two times lower in SiHa than in HCT-116 cells (7 μmol/10^6 cells vs 16 μmol/10^6 cells [28]. In Fig. 3B, we also measured the lactate production that was two times higher in HCT-116 than in SiHa cells. Consequently, the HCT-116 cell line is more glycolytic than the SiHa cell line. We monitored the fate of D-Glucose-$^{13}C_6$ in parental and acid-adapted cells, exposed or not to 5 mM DCA, for lactate and alanine production (Fig. 3A). We observed that the basal lactate production from glucose was significantly lower in acid-adapted cells compared to parental cells (Fig. 3B), confirming that acid-adapted cells are less glycolytic as previously shown in our laboratory [28,29]. When exposed to DCA 5 mM, we observed the expected reduction in lactate production from glucose (Fig. 3A, C). This result was observed in all parental and acid-adapted cancer cells. Interestingly, we observed that the relative decrease in lactate production from glucose was significantly more important in acid-adapted cells than in parental cells (Fig. 3C). In parental HCT-116 cells, we also observed that DCA treatment reduced the production of alanine, a metabolite produced by reductive amination of pyruvate (Fig. 3D). In SiHa cells, the very low basal glycolytic flux prevented the detection of alanine. Finally, an increase in OCR was observed in all cell lines except in SiHa parental cell line. This increase in OCR was more important in acid-adapted cells than in parental cells (Fig. 3E).

3.4. DCA-induced oxidative shift accounts for the growth inhibitory action of DCA through reduction of PPP activity and enhancement of apoptosis

De Preter et al. previously demonstrated that the inhibition of glycolysis by DCA controlled proliferation through reduction in pentose phosphate pathway (PPP) [16]. To bridge this gap between the proliferation assays and glycolytic flux measured in parental and acid-adapted cells, we evaluated the PPP flux by measuring the NADPH/NADP ratio after treatment using DCA and/or using 6-aminonicotamide (6-AN), a specific inhibitor of the PPP [33,34]. We observed that DCA had no influence on NADPH/NADP ratio in parental cells (Fig. 4A), but significantly reduced this ratio in acid-adapted cells. Interestingly, 6-AN also slightly reduced the NADPH/NADP ratio depending on the cell type (Fig. 4A). Most importantly, there was no significant difference between cells treated with DCA or 6-AN. Moreover, no additional decrease was observed when cells were simultaneously exposed to DCA and the PPP inhibitor, 6-AN. Overall, these results suggest that the decrease in NADPH production in acid-adapted cells is linked to a reduction in the PPP.

In addition to DCA anti-proliferative effects, we also observed that DCA exposure led to a decrease in cell density. Therefore, we investigated the effect of DCA exposure on apoptosis and cell death with flow cytometry. 10 mM DCA exposure for 48 h induced an increase in early and late apoptotic cells in acid-adapted HCT-116 cells, but not in parental cells (Fig. 4B–C). In acid-adapted SiHa cells, DCA exposure did not increase the proportion of early apoptotic cells but increased the proportion of late apoptotic/dead cells. In contrast, DCA exposure did not increase early apoptosis nor cell death in SiHa parental cells.

3.5. DCA exposure exacerbates glutamine metabolism in acid-adapted cells

We used L-Glutamine-$^{13}C_5$ tracer to measure glutamine metabolism (glutamate, malate and aspartate production from glutamine) by ^{13}C NMR spectrometry (Fig. 5A). We first observed that the glutamine uptake (determined from residual extracellular glutamine concentration after 24h) was higher in acid-adapted cells than in parental cells (Fig. 5B). Interestingly, for both cell lines the intracellular concentration of glutamine was higher in acid-adapted cells than in parental cells (Fig. 5C). DCA also increased intracellular glutamine concentration in acid-adapted cells but not in parental cells. No significant change in glutamate concentration was observed after DCA treatment, except for HCT-116 acid-adapted cells (Fig. 5D). Contrarily to the effect observed in parental cells, exposure to 5 mM DCA induced a significant increase

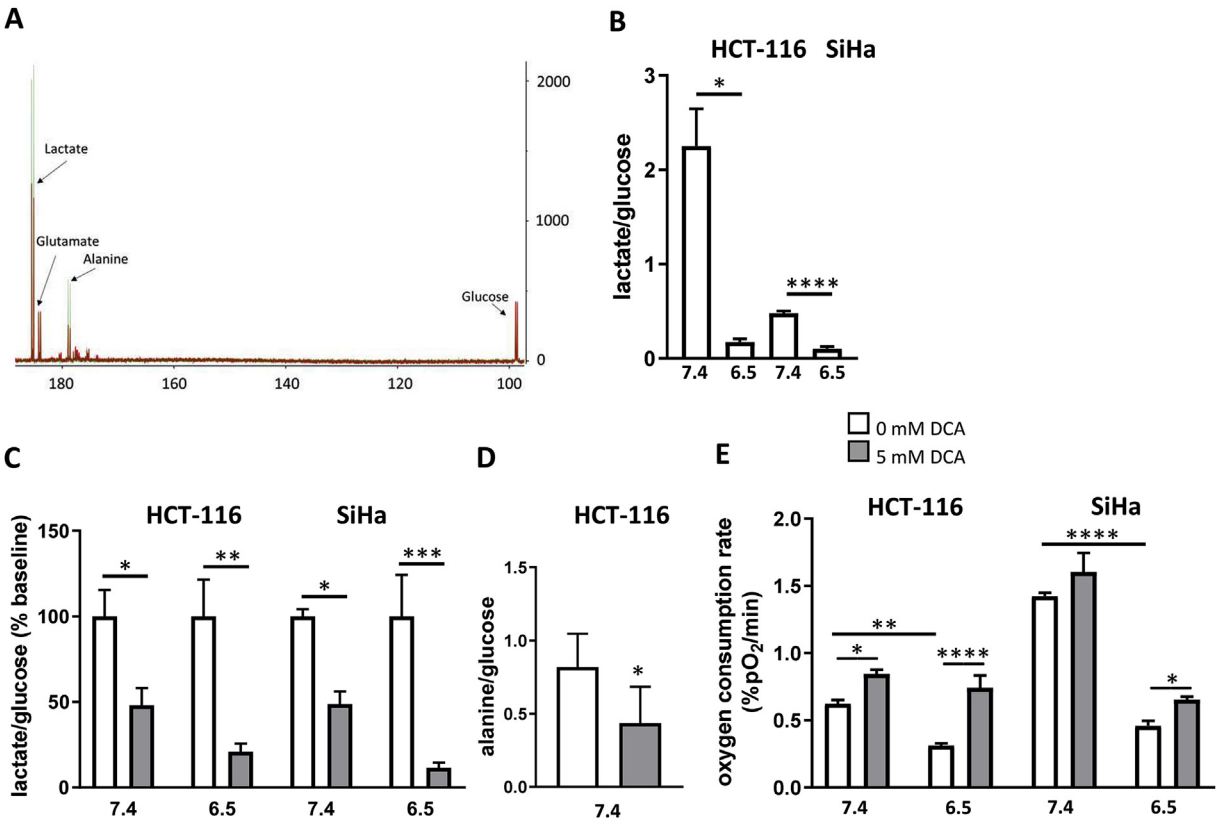

Fig. 3. The "glycolysis to oxidative" shift induced by DCA is larger in acid-adapted cells. A-D, Tumor cells were exposed during 24h to 10 mM of glucose-$^{13}C_6$ with or without 5 mM of DCA. Intra- and extracellular metabolites were measured by ^{13}C NMR spectroscopy (n = 5). A, representative spectra of intracellular metabolites of HCT-116 parental cells with zero (green) or 5 mM of DCA (red). B, lactate production from glucose in control conditions (0 mM DCA); results are expressed as ratio of total lactate (sum of intra-and extracellular lactate) on intracellular glucose. C, Baseline-corrected lactate production from glucose highlighting the larger effect of DCA in acid-adapted cells. D, alanine production from glucose (ratio of intracellular alanine on intracellular glucose). E, Oxygen consumption rate measured in parental HCT – 116, SiHa cell lines and their corresponding acidic-adapted cells, treated with or without 5 mM DCA for 24h (n = 3). Statistical analysis: paired *t*-test (D) and Two-way ANOVA (B, C, E) (Sidak's multiple comparisons test) *p < 0.05, **p < 0.01, ***p < 0.001, ****p < 0. 0001. (For interpretation of the references to colour in this figure legend, the reader is referred to the Web version of this article.)

in malate production from L-Glutamine-$^{13}C_5$ in acid-adapted cells (Fig. 5E). We also observed that the intracellular concentration of aspartate (produced from L-Glutamine-$^{13}C_5$) was increased in parental cells exposed to DCA 5 mM (Fig. 5F). As aspartate is produced by oxaloacetate, an intermediate of TCA cycle, this supports a stimulatory effect of DCA on glutamine metabolism in parental cells maintained at neutral pH. Using ^{13}C NMR, we failed to detect aspartate in acid-adapted cells. Finally, with mass spectrometry, we observed that the production of pyruvate from glutamine, a reaction involving another intermediate of the TCA cycle, namely malate, was more important in acid-adapted SiHa cells compared to parental SiHa cells (Fig. 5G).

3.6. The combination of DCA with a glutaminase inhibitor enhances the cytotoxic effect of DCA in acid-adapted cells

As DCA increased glutamine utilization, we hypothesized that stronger cytotoxic effects could be obtained by the association of DCA to an inhibitor of the glutamine pathway. For this purpose, we combined DCA with BPTES, an inhibitor of glutaminase-1 which converts glutamine into glutamate. We observed that in parental and acid-adapted cells, the combination DCA and BPTES significantly enhanced the growth inhibitory action of DCA (Fig. 6), an effect that was much more pronounced in acid-adapted cells.

4. Discussion

At first sight, the higher DCA-induced toxicity on tumor cells chronically exposed to acidosis compared to parental cells (Fig. 1) looks paradoxical considering that those cells are more prone to use glutamine and fatty acids at the expense of the glycolytic metabolism [28]. This unexpected observation prompted us to dissect the mechanisms responsible for this DCA effect which revealed an exquisite interplay between acidosis, pyruvate dehydrogenase and mitochondria at the origin of this enhanced anti-cancer activity.

We first observed a larger decrease in PDH phosphorylation in acid-adapted cells (Fig. 2A), an effect consistent with the PDK inhibition induced by DCA. Both the higher uptake of DCA and the lower expression of PDK isoforms observed in acid-adapted cells account for this enhanced PDK inhibition (Fig. 2B–C). It has been suggested that the uptake of DCA is mediated by monocarboxylate transporter and traverses the mitochondrial membranes via pyruvate transporter systems [11]. In addition, MCT1 (monocarboxylate transporter 1) is upregulated in tumor cells chronically exposed to acidosis [28]. However, in our case, the MCT1 blocker AR-155858 [35] and the MPC (mitochondrial pyruvate carrier) blocker 7ACC2 [36] did not affect DCA-induced cytotoxicity (data not shown). While DCA is mostly present under the ionized deprotonated form at pH 6.5 and 7.4 (due to its low pKa, 1.35), the proportion of neutral protonated form is about ten times higher at pH 6.5 compared to pH 7.4, a factor that could contribute to a higher diffusion of DCA through the cell membrane. However, the sole increase in DCA uptake cannot account for the increase in toxicity as we did not observe any significant difference in cell density between parental cells under physiological pH and cells acutely exposed to acidic pH under acute acidic (Fig. 1A–B). The increase in DCA concentration

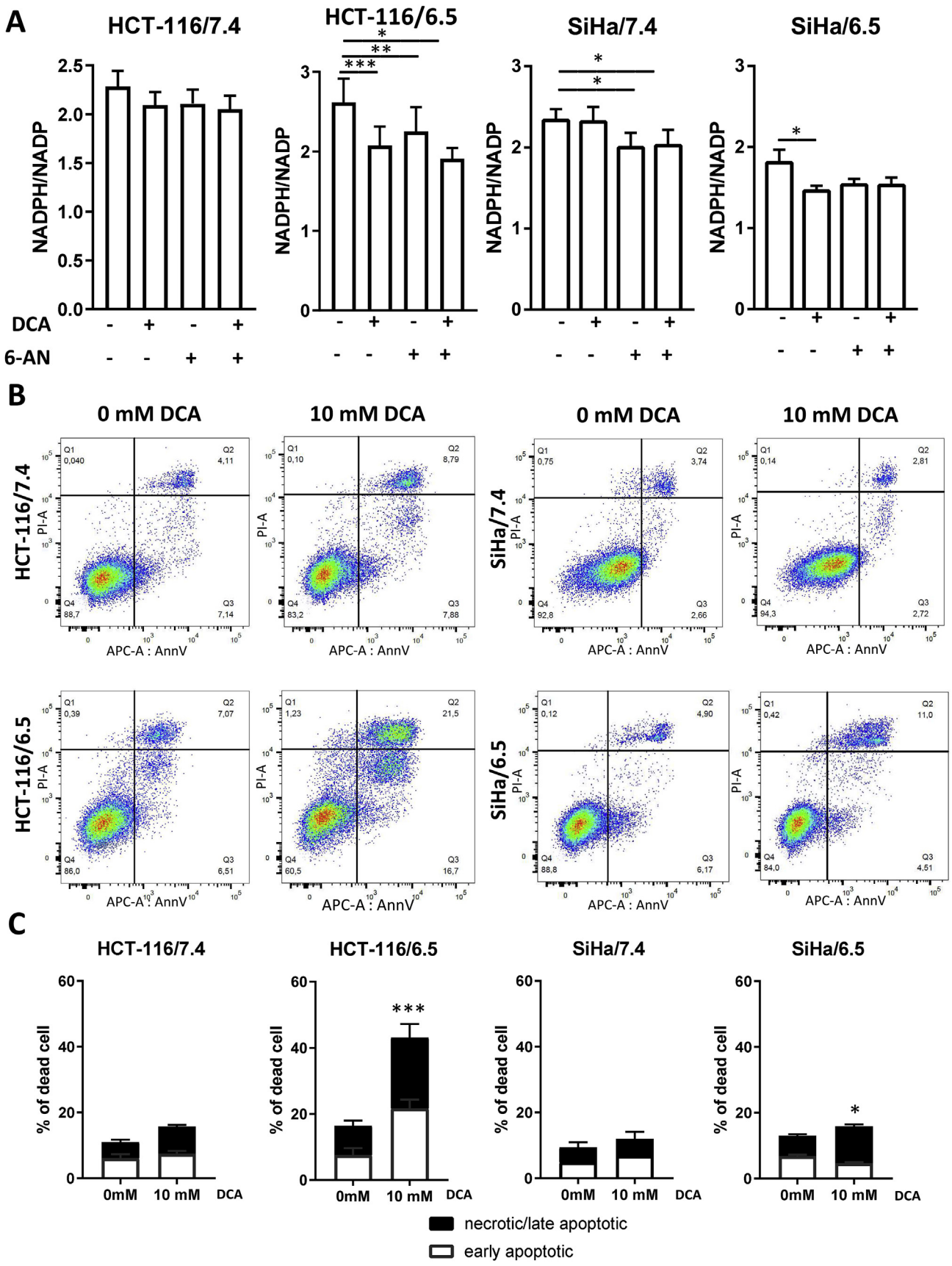

Fig. 4. DCA decreases PPP activity and enhances apoptosis in acid-adapted cells, but not in parental cells. A, NADPH/NADP measurements (n = 3) in HCT - 116, SiHa cell lines and their pH 6.5 – adapted cells treated with or without DCA (5 mM, 48h) and with or without 6-AN (100 μM, 48h). B, representative AnnexinV/PI flow cytometry plots of HCT-116 parental and acid-adapted cells and SiHa parental and acid-adapted cells, treated with or without 10 mM of DCA for 48h. C, histograms of percentage of apoptotic and dead cells. Statistical analysis: One-way (A) or Two-way ANOVA (Sidak's multiple comparison test) (C), *p < 0.05, **p < 0.01, ***p < 0.001.

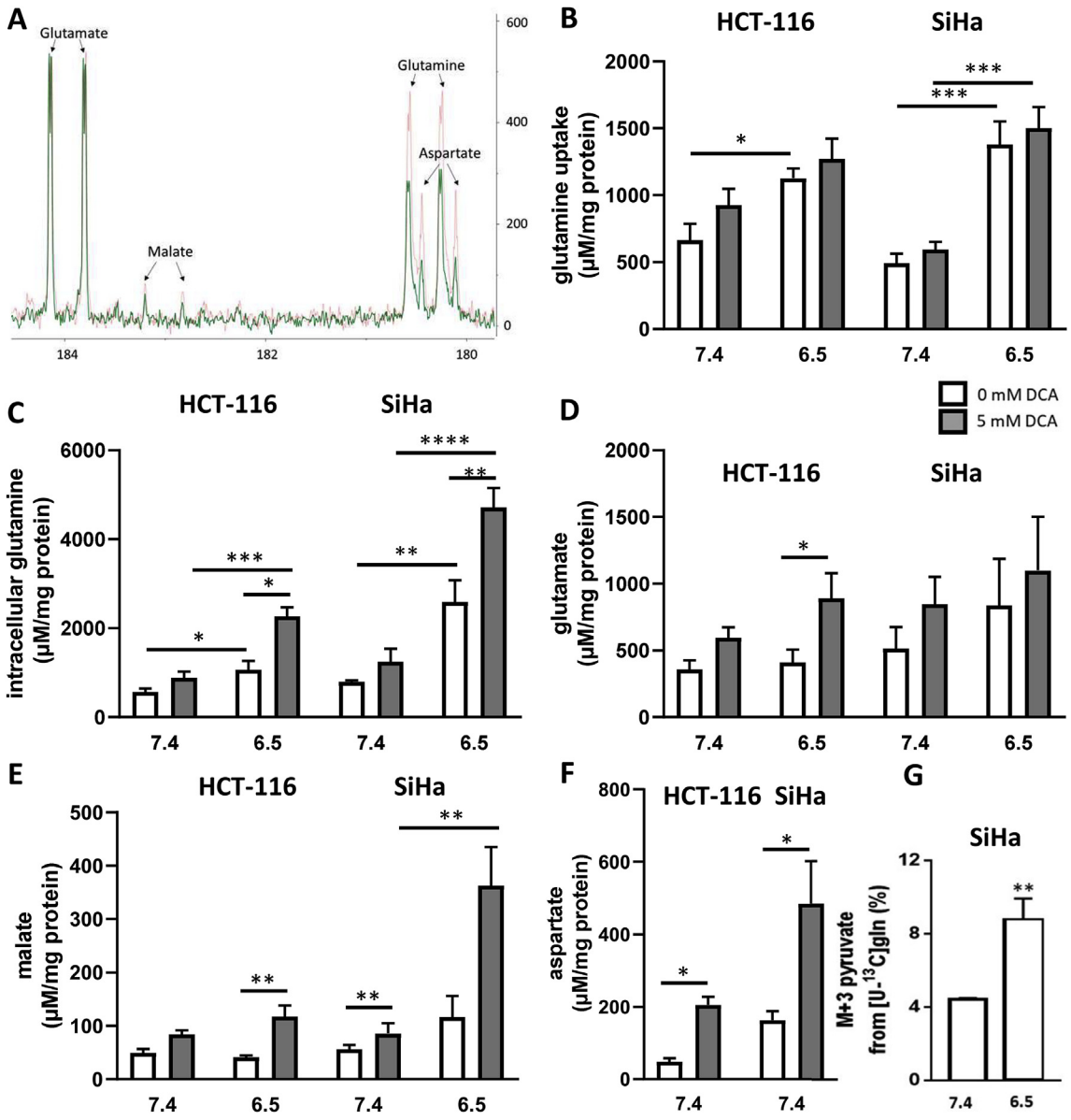

Fig. 5. Glutamine utilization is higher in acid-adapted cells leading to an increase in pyruvate production. A-F, SiHa and HCT-116 tumor cells were exposed during 24h to 2 mM Glutamine-^{13}C5 with or without 5 mM DCA. Intra- and extracellular metabolites were measured by ^{13}C NMR spectroscopy (n = 4) and result were normalize by total protein mass (mg). A, representative spectra of intracellular metabolites of HCT-116 parental cells with zero (green) or 5 mM of DCA (red). B, glutamine uptake. C, intracellular glutamine concentration. D, intracellular glutamate concentration. E, intracellular malate concentration. F, intracellular aspartate concentration. G, relative abundance of pyruvate mass isotopomers in parental and acidic acid-adapted SiHa cells cultured for 72 h with glutamine-5-^{13}C. Statistical analysis: Two-way ANOVA Sidak's multiple comparisons test (B–F) and paired *t*-test (G). *p < 0.05, **p < 0.01, ***p < 0.001, ****p < 0, 0001. (For interpretation of the references to colour in this figure legend, the reader is referred to the Web version of this article.)

coincided with a lower abundance of PDK isoforms observed in acid-adapted cells (Fig. 2C). This downregulation of PDKs could be due to alterations in the transcription factor HIF1-alpha activity. Corbet et al. have indeed previously demonstrated that acid-adapted cells present a downregulation of HIF-1 alpha [28] and other studies have shown that PDK1 and PDK3 are upregulated by HIF-1 alpha [37–39]. To our knowledge, the regulation of PDK2 and PDK4 by HIF-1 alpha has not been studied yet. The decrease in target enzyme together with higher concentration of the inhibitor may easily explain the larger decrease in PDH phosphorylation, a phenomenon usually associated with the re-activation of the transformation of pyruvate into acetyl-CoA. In our study, although the basal production of lactate was lower in acid-adapted cells compared to parental cells (Fig. 3B), we found that DCA induced a larger decrease in glycolytic flux (i.e., a larger relative reduction in lactate/glucose ratio) and an increase in oxidative phosphorylation (as evidenced by a net increase in OCR) in acid-adapted cells (Fig. 3). One may thus hypothesize that the low residual glycolytic metabolism in acid-adapted cancer cells renders them highly sensitive to the effects of DCA that completely shifts the glucose metabolism towards oxidative phosphorylation.

We further analyzed the consequences of this metabolic shift on cell proliferation and viability. It has been previously demonstrated that DCA controlled proliferation through reduction in PPP activity in MDA-MB-231 cell line [16]. DCA decreased PPP activity in acid-adapted cells, but not in parental cell lines (Fig. 4A), an effect that is consistent with the anti-proliferative effect of DCA in acid-adapted cells. Moreover, DCA has been described as a reactivator of mitochondrial apoptosis. By increasing the flux of pyruvate into the TCA cycle, it has been demonstrated that DCA enhanced mitochondrial membrane depolarization, which resulted in a release of pro-apoptotic mediators in the

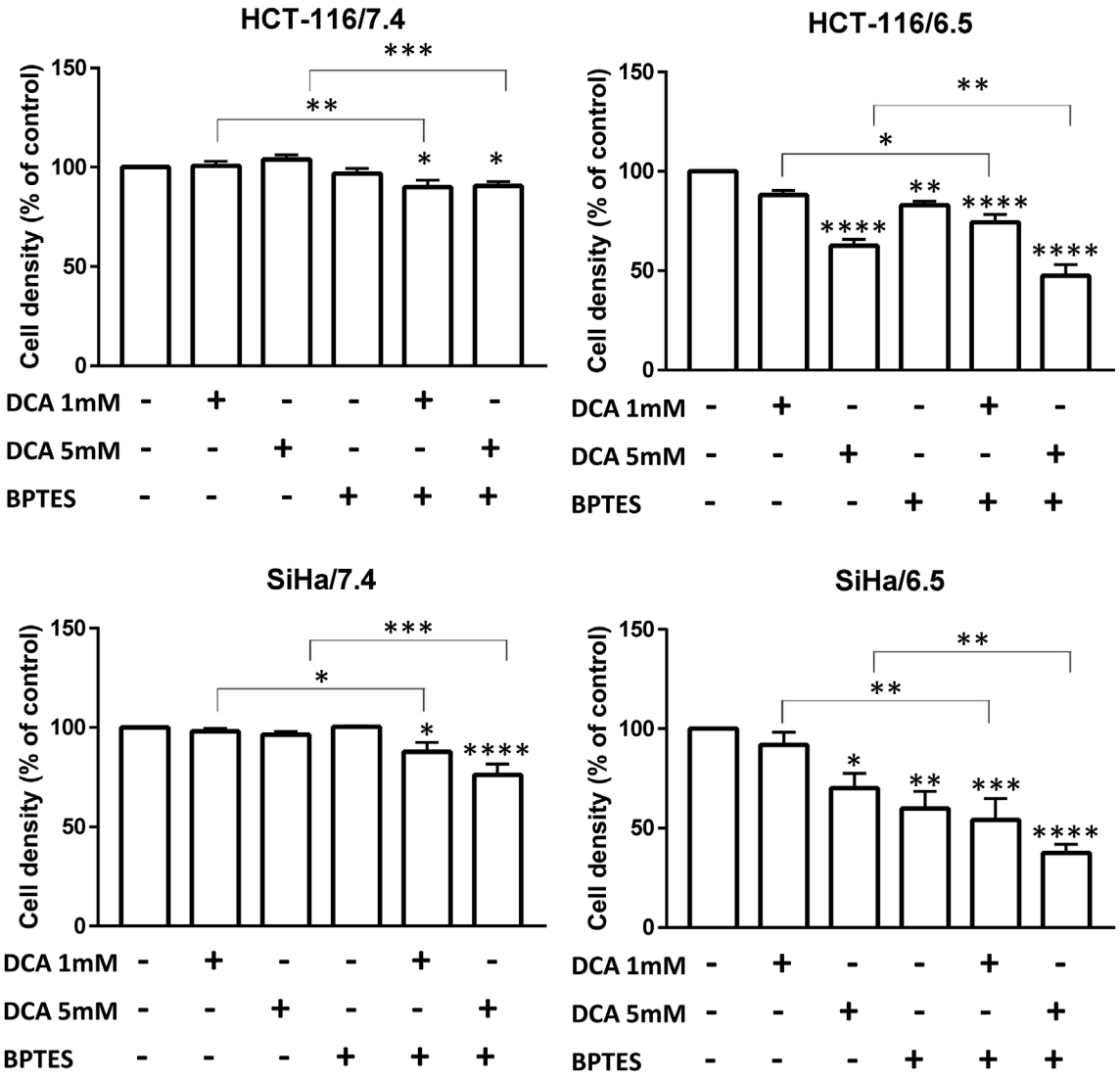

Fig. 6. Combined exposure to DCA and glutaminase inhibitor BPTES decreases tumor cell density more effectively in acid-adapted cells. SiHa and HCT-116 cells were exposed during 48h to increasing doses of DCA (0-1-5-mM) with or without 10 μM of BPTES (n = 3). Statistical analysis: One-way ANOVA Sidak's multiple comparisons test. *p < 0.05, **p < 0.01, ***p < 0.001, ****p < 0, 0001.

cytoplasm [12]. Here, we observed that DCA induced an increase in early and late apoptotic cells in acid-adapted cells (Fig. 4B–C), but not in parental cells. Altogether, these data suggest that DCA exacerbates the glycolytic to oxidative shift observed in acid-adapted cells, thereby decreasing the PPP flux, and reactivates mitochondrial-dependent apoptosis in these cancer cells that are intrinsically dependent on mitochondrial OXPHOS for growth and survival.

Because it has been reported that chronic exposure of tumor cells to acidosis is responsible for a higher dependency toward glutamine utilization [28], we also investigated the effect of DCA treatment on the glutamine pathway. As expected, the uptake of ^{13}C-glutamine was higher in acid-adapted cells (Fig. 5B). The increase in intracellular glutamine concentration in acid-adapted (Fig. 5C) cells as well as pyruvate production from glutamine (Fig. 5G) support the concept that chronic exposure to acidosis leads to an increase in glutamine metabolism via TCA cycling. In acid-adapted cells, we also found that DCA increased the intracellular concentration of glutamine, glutamate and malate in agreement with the DCA-based stimulation of the TCA cycle (Fig. 5C–E). We also found that DCA increased the aspartate production from glutamine in parental cells, in agreement with the DCA-based stimulation of the TCA cycle generating oxaloacetate, the aspartate precursor (Fig. 5F). The failure to detect aspartate in acid-adapted cancer cells suggests that its use to generate purine is by far higher than its production under acidosis. This may arise from a decreased TCA cycle turnover associated to the reduced glucose metabolism in acid-adapted cancer cells. The increased uptake of glutamine could thus reflect an attempt to compensate this alteration as supported by the anaplerotic formation of pyruvate from glutamine (Fig. 5G). This model also supports why the exacerbation of this process in DCA-treated acid-adapted cancer cells, as evidenced by the increased glutamine uptake, makes these cells particularly sensitive to glutaminase inhibitor BPTES (Fig. 6). The interaction between DCA and glutaminase inhibitor deserves to be studied more profoundly and the benefit of this combination should be investigated *in vivo* in order to open new perspectives for combined therapy.

In conclusion, the metabolic reprogramming induced by acidosis sensitizes cancer cells to DCA (Fig. 7) by stimulating apoptosis and thereby opens new perspectives of treatment as monotherapy but also in combination with glutaminase inhibitors since DCA exposure also exacerbates cancer cell addiction towards glutamine metabolism.

Author contribution

Conception and design: C. Schoonjans, B. Gallez.

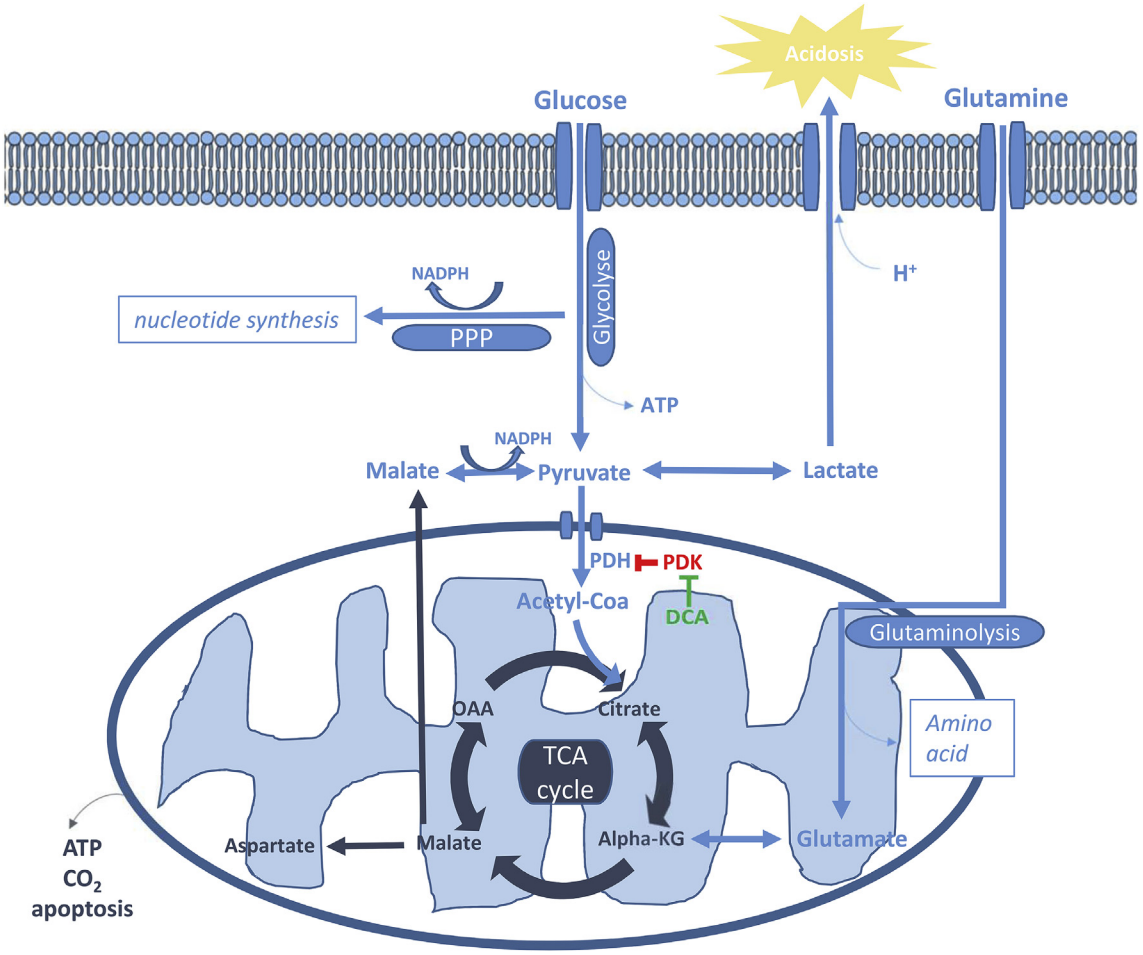

Fig. 7. Effect of DCA and acidosis on bioenergetics of cancer cells. Glucose metabolism through glycolysis produces ATP and carbon intermediates to sustain proliferation such as intermediates for the pentose phosphate pathway (PPP). PPP generates NADPH (defence against ROS) and is involved in nucleotide synthesis. The end-product of glycolysis, pyruvate, can be converted into lactate or acetyl-coA. Acetyl-coA fuels TCA cycle and lactate is exported outside of the cells with one proton and participate to the acidification of extracellular media. TCA cycle produces carbon intermediates for cellular proliferation such as aspartate, glutamate and precursors for lipid synthesis. Malate, through malic enzyme, is converted into pyruvate with generation of NADPH. In the presence of oxygen, TCA cycle via oxidative phosphorylation (OXPHOS) produces ATP. TCA cycle can also be replenished by glutamate. Glutamate is the result of glutaminolysis also involved in amino acid synthesis. In cells exposed to acidosis, DCA increases substrates fueling the TCA cycle by reactivating the PDH and increasing the glutamine utilization.

Development of methodology: C. Schoonjans, N. Joudiou, C. Corbet, D. Brusa.

Acquisition of data: C. Schoonjans.

Analysis and interpretation of data: C. Schoonjans, N. Joudiou, D. Brusa, C. Corbet, O. Feron, B. Gallez.

Writing, review, and/or revision of the manuscript: C. Schoonjans, N. Joudiou, D. Brusa, C. Corbet, O. Feron, B. Gallez.

Study supervision: B. Gallez, O. Feron.

Funding sources

Foundation against Cancer (2015-144 and 2016-087).

C. Schoonjans is a Televie PhD student.

The study used the facilities of the Nuclear and Electronic Spin Technologies (NEST) and Flow Cytometry platforms of UCLouvain.

Declaration of competing interest

The authors declare no potential conflicts of interest.

References

[1] R.J. DeBerardinis, N.S. Chandel, Fundamentals of cancer metabolism, Sci. Adv. 2 (2016) e1600200.

[2] I. Elia, G. Doglioni, S.M. Fendt, Metabolic hallmarks of metastasis formation, Trends Cell Biol. 28 (2018) 673–684.

[3] P.E. Porporato, S. Dhup, R.K. Dadhich, T. Copetti, P. Sonveaux, Anticancer targets in the glycolytic metabolism of tumors: a comprehensive review, Front. Pharmacol. 2 (2011) 49.

[4] R.A. Gatenby, R.J. Gillies, Why do cancers have high aerobic glycolysis? Nat. Rev. Cancer 4 (2004) 891–899.

[5] X.S. Chen, L.Y. Li, Y.D. Guan, J.M. Yang, Y. Cheng, Anticancer strategies based on the metabolic profile of tumor cells: therapeutic targeting of the Warburg effect, Acta Pharmacol. Sin. 37 (2016) 1013–1019.

[6] S. Fortunato, G. Bononi, C. Granchi, F. Minutolo, An update on patents covering agents that interfere with the cancer glycolytic cascade, ChemMedChem 13 (2018) 2251–2265.

[7] T. Golias, M. Kery, S. Radenkovic, I. Papandreou, Microenvironmental control of glucose metabolism in tumors by regulation of pyruvate dehydrogenase, Int. J. Cancer 144 (2019) 674–686.

[8] E. Saunier, C. Benelli, S. Bortoli, The pyruvate dehydrogenase complex in cancer: an old metabolic gatekeeper regulated by new pathways and pharmacological agents, Int. J. Cancer 138 (2016) 809–817.

[9] G. Kroemer, J. Pouyssegur, Tumor cell metabolism: cancer's Achilles' heel, Cancer Cell 13 (2008) 472–482.

[10] S. Bonnet, S.L. Archer, J. Allalunis-Turner, A. Haromy, C. Beaulieu, R. Thompson, C.T. Lee, G.D. Lopaschuk, L. Puttagunta, S. Bonnet, G. Harry, K. Hashimoto, C.J. Porter, M.A. Andrade, B. Thebaud, E.D. Michelakis, A mitochondria-K+ channel axis is suppressed in cancer and its normalization promotes apoptosis and inhibits cancer growth, Cancer Cell 11 (2007) 37–51.

[11] S. Kankotia, P.W. Stacpoole, Dichloroacetate and cancer: new home for an orphan drug? Biochim. Biophys. Acta 1846 (2014) 617–629.

[12] G. Sutendra, E.D. Michelakis, Pyruvate dehydrogenase kinase as a novel therapeutic

target in oncology, Front. Oncol. 3 (2013) 38.
[13] E.M. Dunbar, B.S. Coats, A.L. Shroads, T. Langaee, A. Lew, J.R. Forder, J.J. Shuster, D.A. Wagner, P.W. Stacpoole, Phase 1 trial of dichloroacetate (DCA) in adults with recurrent malignant brain tumors, Investig. New Drugs 32 (2014) 452–464.
[14] Q.S. Chu, R. Sangha, J. Spratlin, L.J. Vos, J.R. Mackey, A.J. McEwan, P. Venner, E.D. Michelakis, A phase I open-labeled, single-arm, dose-escalation, study of dichloroacetate (DCA) in patients with advanced solid tumors, Investig. New Drugs 33 (2015) 603–610.
[15] E.D. Michelakis, L. Webster, J.R. Mackey, Dichloroacetate (DCA) as a potential metabolic-targeting therapy for cancer, Br. J. Canc. 99 (2008) 989–994.
[16] G. De Preter, M.A. Neveu, P. Danhier, L. Brisson, V.L. Payen, P.E. Porporato, B.F. Jordan, P. Sonveaux, B. Gallez, Inhibition of the pentose phosphate pathway by dichloroacetate unravels a missing link between aerobic glycolysis and cancer cell proliferation, Oncotarget 7 (2016) 2910–2920.
[17] G. Sutendra, P. Dromparis, A. Kinnaird, T.H. Stenson, A. Haromy, J.M. Parker, M.S. McMurtry, E.D. Michelakis, Mitochondrial activation by inhibition of PDKII suppresses HIF1a signaling and angiogenesis in cancer, Oncogene 32 (2013) 1638–1650.
[18] M. Morfouace, L. Lalier, M. Bahut, V. Bonnamain, P. Naveilhan, C. Guette, L. Oliver, N. Gueguen, P. Reynier, F.M. Vallette, Comparison of spheroids formed by rat glioma stem cells and neural stem cells reveals differences in glucose metabolism and promising therapeutic applications, J. Biol. Chem. 287 (2012) 33664–33674.
[19] I. Papandreou, T. Goliasova, N.C. Denko, Anticancer drugs that target metabolism: is dichloroacetate the new paradigm? Int. J. Cancer 128 (2011) 1001–1008.
[20] J.W. Wojtkowiak, D. Verduzco, K.J. Schramm, R.J. Gillies, Drug resistance and cellular adaptation to tumor acidic pH microenvironment, Mol. Pharm. 8 (2011) 2032–2038.
[21] K.M. Bailey, J.W. Wojtkowiak, A.I. Hashim, R.J. Gillies, Targeting the metabolic microenvironment of tumors, Adv. Pharmacol. 65 (2012) 63–107.
[22] M. Damaghi, N.K. Tafreshi, M.C. Lloyd, R. Sprung, V. Estrella, J.W. Wojtkowiak, D.L. Morse, J.M. Koomen, M.M. Bui, R.A. Gatenby, R.J. Gillies, Chronic acidosis in the tumour microenvironment selects for overexpression of LAMP2 in the plasma membrane, Nat. Commun. 6 (2015) 8752.
[23] M. Damaghi, R. Gillies, Phenotypic changes of acid-adapted cancer cells push them toward aggressiveness in their evolution in the tumor microenvironment, Cell Cycle 16 (2017) 1739–1743.
[24] V. Estrella, T. Chen, M. Lloyd, J. Wojtkowiak, H.H. Cornnell, A. Ibrahim-Hashim, K. Bailey, Y. Balagurunathan, J.M. Rothberg, B.F. Sloane, J. Johnson, R.A. Gatenby, R.J. Gillies, Acidity generated by the tumor microenvironment drives local invasion, Cancer Res. 73 (2013) 1524–1535.
[25] S.R. Pillai, M. Damaghi, Y. Marunaka, E.P. Spugnini, S. Fais, R.J. Gillies, Causes, consequences, and therapy of tumors acidosis, Cancer Metastasis Rev. (2019).
[26] G. Lamonte, X. Tang, J.L. Chen, J. Wu, C.K. Ding, M.M. Keenan, C. Sangokoya, H.N. Kung, O. Ilkayeva, L.G. Boros, C.B. Newgard, J.T. Chi, Acidosis induces reprogramming of cellular metabolism to mitigate oxidative stress, Cancer Metabol. 1 (2013) 23.
[27] C. Corbet, O. Feron, Tumour acidosis: from the passenger to the driver's seat, Nat. Rev. Cancer 17 (2017) 577–593.
[28] C. Corbet, N. Draoui, F. Polet, A. Pinto, X. Drozak, O. Riant, O. Feron, The SIRT1/HIF2alpha axis drives reductive glutamine metabolism under chronic acidosis and alters tumor response to therapy, Cancer Res. 74 (2014) 5507–5519.
[29] C. Corbet, A. Pinto, R. Martherus, J.P. Santiago de Jesus, F. Polet, O. Feron, Acidosis drives the reprogramming of fatty acid metabolism in cancer cells through changes in mitochondrial and histone acetylation, Cell Metabol. 24 (2016) 311–323.
[30] O. Feron, L. Belhassen, L. Kobzik, T.W. Smith, R.A. Kelly, T. Michel, Endothelial nitric oxide synthase targeting to caveolae. Specific interactions with caveolin isoforms in cardiac myocytes and endothelial cells, J. Biol. Chem. 271 (1996) 22810–22814.
[31] Q. Teng, W. Huang, T.W. Collette, D.R. Ekman, C. Tan, A direct cell quenching method for cell-culture based metabolomics, Metabolomics 5 (2008) 199.
[32] B.F. Jordan, V. Gregoire, R.J. Demeure, P. Sonveaux, O. Feron, J. O'Hara, V.P. Vanhulle, N. Delzenne, B. Gallez, Insulin increases the sensitivity of tumors to irradiation: involvement of an increase in tumor oxygenation mediated by a nitric oxide-dependent decrease of the tumor cells oxygen consumption, Cancer Res. 62 (2002) 3555–3561.
[33] D.A. Scott, A.D. Richardson, F.V. Filipp, C.A. Knutzen, G.G. Chiang, Z.A. Ronai, A.L. Osterman, J.W. Smith, Comparative metabolic flux profiling of melanoma cell lines: beyond the Warburg effect, J. Biol. Chem. 286 (2011) 42626–42634.
[34] E. Tsouko, A.S. Khan, M.A. White, J.J. Han, Y. Shi, F.A. Merchant, M.A. Sharpe, L. Xin, D.E. Frigo, Regulation of the pentose phosphate pathway by an androgen receptor-mTOR-mediated mechanism and its role in prostate cancer cell growth, Oncogenesis 3 (2014) e103.
[35] M.J. Ovens, A.J. Davies, M.C. Wilson, C.M. Murray, A.P. Halestrap, AR-C155858 is a potent inhibitor of monocarboxylate transporters MCT1 and MCT2 that binds to an intracellular site involving transmembrane helices 7-10, Biochem. J. 425 (2010) 523–530.
[36] C.V. Linden, C. Corbet, Killing two birds with one stone: blocking the mitochondrial pyruvate carrier to inhibit lactate uptake by cancer cells and radiosensitize tumors, Mol. Cell. Oncol. 5 (2018) e1465016.
[37] C.W. Lu, S.C. Lin, K.F. Chen, Y.Y. Lai, S.J. Tsai, Induction of pyruvate dehydrogenase kinase-3 by hypoxia-inducible factor-1 promotes metabolic switch and drug resistance, J. Biol. Chem. 283 (2008) 28106–28114.
[38] H. Semba, N. Takeda, T. Isagawa, Y. Sugiura, K. Honda, M. Wake, H. Miyazawa, Y. Yamaguchi, M. Miura, D.M. Jenkins, H. Choi, J.W. Kim, M. Asagiri, A.S. Cowburn, H. Abe, K. Soma, K. Koyama, M. Katoh, K. Sayama, N. Goda, R.S. Johnson, I. Manabe, R. Nagai, I. Komuro, HIF-1alpha-PDK1 axis-induced active glycolysis plays an essential role in macrophage migratory capacity, Nat. Commun. 7 (2016) 11635.
[39] N. Ho, B.L. Coomber, Pyruvate dehydrogenase kinase expression and metabolic changes following dichloroacetate exposure in anoxic human colorectal cancer cells, Exp. Cell Res. 331 (2015) 73–81.